Effective transport properties of random composites: Continuum calculations versus mapping to a network

PHYSICAL REVIEW E **80**, 040103(R) (2009)

Effective transport properties of random composites: Continuum calculations versus mapping to a network

Ying Chen and Christopher A. Schuh*

Department of Materials Science and Engineering, Massachusetts Institute of Technology, 77 Massachusetts Avenue, Cambridge, Massachusetts 02139, USA

(Received 10 August 2009; published 16 October 2009)

The effective transport properties and percolation of continuum composites have commonly been studied using discrete models, i.e., by mapping the continuum to a lattice or network. In this study we instead directly solve the continuum transport equations for composite microstructures both analytically and numerically, and we extract the continuum percolation threshold and scaling exponents for the two-dimensional square tile system. We especially focus on the role of corner contacts on flux flow and further show that mapping such "random checkerboard" systems to a network leads to a spurious secondary percolation threshold and causes shifts in the critical scaling exponents of the effective transport properties.

DOI: 10.1103/PhysRevE.80.040103 PACS number(s): 64.60.ah, 62.23.Pq, 87.16.dp

The macroscopic effective transport properties of continuum composites [1,2]—such as electrical and thermal conductivities, mass diffusivity, or permeability—are largely determined by phase connectivity and percolation [3–5]. Percolation effects, however, have not been successfully incorporated in traditional homogenization schemes, e.g., effective-medium theories [6], for continuum composites, mainly due to the lack of understanding of continuum percolation for transport processes. Existing studies on continuum percolation for the most part have not rigorously considered transport through the continuum, *per se*, but instead mapped the phase connectivity to a discrete network or lattice [7–10]. The mapping approach entirely relies on a connectivity criterion decided beforehand, e.g., whether phase domain contacts at corners (as well as edge contacts in three dimensions) are deemed valid transport paths and what local transport coefficients to assign to these "secondary" contacts. One recent study used finite element analysis to solve for the effective conductivities of composite microstructures, but only after applying a corner contact rule similar to those described above on discrete lattices [11]. To the authors' knowledge, to date there has not been any work systematically studying continuum percolation of transport processes by strictly solving continuum transport equations on the original continuum microstructure, nor has there been any detailed study of the viability of secondary contacts as continuum transport paths. It is the purpose of this Rapid Communication to take some steps in approaching this open problem by analytical derivation and large-scale numerical calculations. We find that mapping continuum composites onto discrete networks will, in general, not yield correct effective transport properties and percolation parameters, and we attribute the discrepancy to strong variations in transport fields around geometric irregularities, i.e., secondary contacts in the present context, that mapped regular networks cannot capture.

We begin by elucidating how transport occurs at corner contacts for a simple two-dimensional example. Consider the quartered geometry shown in Fig. 1(a) with corner contacts between regions (ii) and (iii) of phase 1 and between regions (i) and (iv) of phase 2, with perfect bonding everywhere. Working in the context of mass diffusion, we assign phase 1 a low diffusivity D_1 and phase 2 a higher diffusivity D_2, and we relate the diffusion flux J to the concentration C by Fick's first law. Solving the Laplace equation for steady state and further requiring C and the normal component of J to be continuous across phase boundaries leads to an analytical form for the concentration field $C=C_0+\Sigma H_\mu C_\mu$, where the summation runs over all values permitted by the definition of μ [as given below in Eq. (2)], H_μ are constants to be determined by external boundary conditions (which are irrelevant for the present discussion), and C_μ, expressed in polar coordinates, is

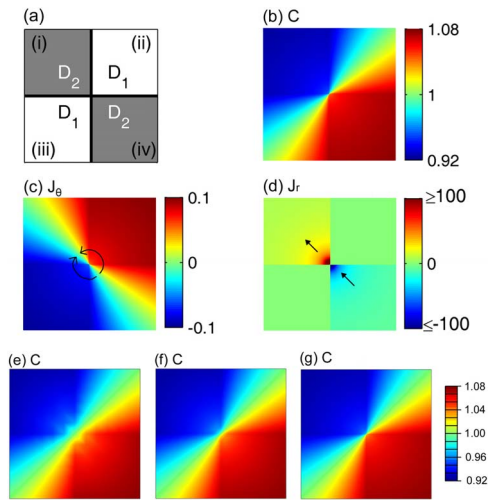

FIG. 1. (Color online) (a) Schematic of a corner-corner contact in a square domain ($-0.1\leq x$ and $y\leq 0.1$) with phases 1 and 2 assigned diffusivities $D_1=1$ and $D_2=100$. (b), (c), and (d) are the distributions of concentration $C=1+C_{\mu_0}$, angular flux $J_{\theta\mu_0}$, and radial flux $J_{r\mu_0}$, respectively, calculated from Eq. (1). (e)–(g) show the concentration distribution C from continuum FEM calculations with gradually refined mesh sizes [total elements used increases from 36 in (e) to 66 in (f) and 250 in (g)].

*Corresponding author; schuh@mit.edu

$$C_\mu(r,\theta) = \begin{cases} -r^\mu \sin\left(\frac{\pi}{4}\mu\right)\cos\left[\left(\theta-\frac{3\pi}{4}\right)\mu\right], & \theta\in\left[\frac{\pi}{2},\pi\right] \text{ in (i)} \\ -r^\mu \cos\left(\frac{\pi}{4}\mu\right)\sin\left[\left(\theta-\frac{\pi}{4}\right)\mu\right], & \theta\in\left[0,\frac{\pi}{2}\right] \text{ in (ii)} \\ +r^\mu \cos\left(\frac{\pi}{4}\mu\right)\sin\left[\left(\theta+\frac{3\pi}{4}\right)\mu\right], & \theta\in\left[-\pi,-\frac{\pi}{2}\right] \text{ in (iii)} \\ +r^\mu \sin\left(\frac{\pi}{4}\mu\right)\cos\left[\left(\theta+\frac{\pi}{4}\right)\mu\right], & \theta\in\left[-\frac{\pi}{2},0\right] \text{ in (iv)}, \end{cases} \tag{1}$$

with

$$\mu = \frac{2}{\pi}\arcsin\left(\frac{2\sqrt{D_1D_2}}{D_1+D_2}\right) + 4n = \mu_0 + 4n, \quad n = 0,1,2,\ldots, \tag{2}$$

where μ_0 lies between 0 and 1. The angular and the radial components of flux are $J_{\theta\mu}=-D\partial C_\mu/\partial\theta\propto r^\mu$ and $J_{r\mu}=-D\partial C_\mu/\partial r\propto r^{\mu-1}$. As $r\to 0$, $J_{\theta\mu_0}$ and $J_{r\mu_0}$ become the dominant flux terms ($J_{r\mu_0}$ in fact diverges) as all other $J_{\theta\mu_n}$ and $J_{r\mu_n}$ with $n>0$ vanish in the limit. The distributions of $C=1+C_{\mu_0}$, $J_{\theta\mu_0}$, and $J_{r\mu_0}$ very near the corner are shown in Figs. 1(b)–1(d), respectively. Flux flows around the corner in phase 1, as shown in Fig. 1(c), and also across the corner-corner contact of phase 2, as illustrated by arrows in Fig. 1(d). We determine the local effective diffusivity D_{eff} of a circular region with radius R surrounding the corner contact using the distributions of C, $J_{\theta\mu_0}$, and $J_{r\mu_0}$,

$$D_{\text{eff}} = -\frac{\langle J\rangle}{\langle\nabla C\rangle} = \frac{\mu_0^2 R+\mu_0+1}{\mu_0^2+\mu_0 R+\mu_0}\sqrt{D_1D_2} \overset{R\to 0}{\to} \frac{1}{\mu_0}\sqrt{D_1D_2}. \tag{3}$$

This nonzero local effective diffusivity verifies that diffusion can occur across corner contacts from a continuum perspective. A well-known corroboration of the above result can be found in the regular checkerboard microstructure, which is a periodic distribution of the square domain in Fig. 1(a). Many theoretical studies founded on symmetry arguments have shown that the effective transport coefficient of a regular checkerboard is the geometric mean of those of the two phases, i.e., $D_{\text{eff}}=\sqrt{D_1D_2}$ [12–18]. Since only corner contacts provide phase contiguity in the checkerboard, this value of D_{eff} suggests that corner contacts must allow for diffusive flow; otherwise, D_{eff} for discontinuous composites would instead be close to the Hashin-Shtrikman lower bound [19,20].

Consider a related microstructure: the so-called random checkerboard generated by assigning square tiles randomly as either phase 1 or 2. Sheng and Kohn [21] evaluated the effective dielectric constant ε_{eff} of a random checkerboard by assuming that a local effective dielectric constant of $\sqrt{\varepsilon_1\varepsilon_2}$ would apply at each corner contact, and then using the effective-medium approach [22]. The resulting ε_{eff} exhibits two percolation thresholds at $p_c=0.449$ and 0.551, with the former being attributed to the emergence of a percolation cluster relying on both corner and edge contacts and the latter being attributed to the formation of a percolation cluster fully connected through edges. Later, Nettelblad *et al.* [23] as well as Martensson and Gafvert [24,25] mapped the three-dimensional random checkerboard onto a network, with edge contacts between two σ_2 cubes replaced with bonds with conductivity $\sqrt{\sigma_1\sigma_2}$ and corner contacts neglected. By solving the Kirchhoff equations for the network, they also observed two percolation thresholds for the effective conductivity. However, we note that the continuum transport in the vicinity of an individual corner or edge contact in random checkerboards depends on more details of the nearby phase distributions and should be different from that in a regular checkerboard. We therefore do not expect that the geometric mean can be strictly applied at corners in random checkerboards and suggest that prior observations of two percolation thresholds and the associated percolation properties reported by such studies may not be truly relevant for the problem of continuum transport. To explore this hypothesis further, we now directly calculate continuum effective diffusivities using the finite element method (FEM) and compare with results obtained from the network mapping procedure.

We first run test calculations on the domain containing four cells shown in Fig. 1(a). The concentration on external surfaces is required to be the same as that in Fig. 1(b), and the concentration in the domain interior is solved in the commercial finite element solver ABAQUS using quadratic elements. The model is remeshed adaptively several times according to previous solution distributions to progressively reduce the element size near the corner; the resulting mesh is highly nonuniform with extremely small elements at corner contacts. Figures 1(e)–1(g) show that, with finer meshes, the concentration distribution converges to the analytical result in Fig. 1(b), confirming that such FEM calculations can capture transport processes in complex microstructures with corner contacts.

We next apply the same FEM technique (with adaptive remeshing) to 100×100 random checkerboards. We apply a high diffusivity contrast ratio, $D_2/D_1=10^8$, in order to clearly reveal the percolation transition. The diffusant concentration is set to be a constant C_0 on the left surface and zero on the right, while a zero-flux condition is imposed at the top and bottom. The calculated effective diffusivities D_{eff} are plotted against p, the fraction of the phase with diffusivity D_2, in Fig. 2(a) as red circles. The abrupt increase in D_{eff} signifies a percolation transition, which occurs only once across the entire range of p. We obtain the percolation probability $\Pi(p)$ by considering the system "percolating" when $D_{\text{eff}}>\sqrt{D_1D_2}$ and otherwise "not percolating" and averaging over many microstructure realizations at the same p. As $d\Pi/dp$ is a Gaussian distribution with a standard deviation Δ [26], integrating $d\Pi/dp$ from 0 to p gives

$$\Pi(p) = \frac{1}{2}\text{erf}\left(\frac{p_c}{\sqrt{2}\Delta}\right) + \frac{1}{2}\text{erf}\left(\frac{p-p_c}{\sqrt{2}\Delta}\right). \tag{4}$$

Fitting $\Pi(p)$ from our numerical calculations to Eq. (4), as shown in the inset in Fig. 2(a), yields the percolation threshold $p_c\approx 0.407$. This value matches that expected for geometric site percolation on random square lattices when next-nearest neighbors are included as connected [27,28]. Thus, in agreement with our earlier discussion, corner contacts are legitimate continuum transport paths, connecting next-nearest neighbors as far as transport properties are concerned

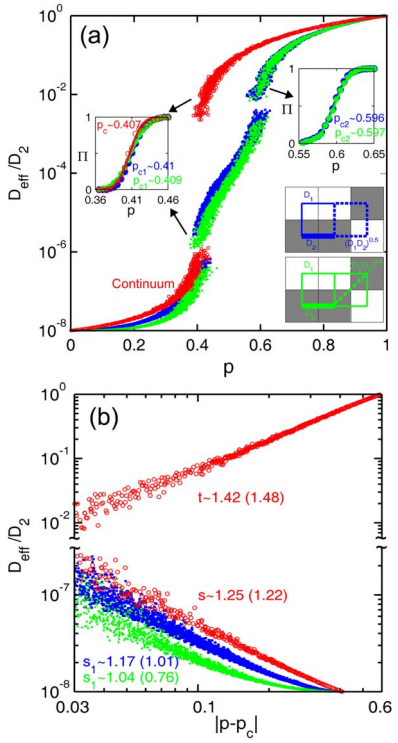

FIG. 2. (Color online) (a) Effective diffusivity D_{eff} of random checkerboards normalized by the diffusivity D_2 of phase 2 as a function of the fraction p of phase 2. The data points plotted as red hollow circles are FEM results for the continuum microstructure, while the solid points plotted in blue (dark gray) and green (light gray) are from two network mapping approaches illustrated in the bottom insets. In these insets, gray tiles are phase 2 and white tiles are phase 1; thick lines represent bonds with diffusivity D_2, thin lines D_1, and dashed lines $\sqrt{D_1 D_2}$. The top insets are the percolation probability Π extracted from the numerical FEM calculations and fitted to Eq. (4). (b) Scaling analysis of the same data, with exponents s and t fitted within the range $0.03 \leq |p-p_c| \leq 0.2$; the values in parentheses are the exponents fitted on the whole curve.

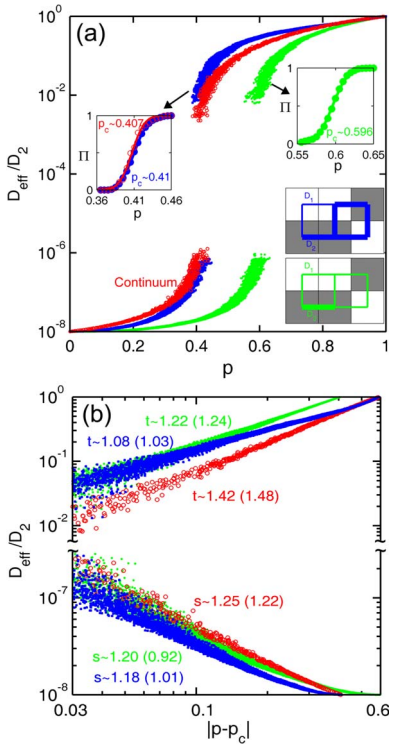

FIG. 3. (Color online) (a) D_{eff} of random checkerboards normalized by the diffusivity D_2 of phase 2 as a function of the fraction p of phase 2. The data points plotted as red hollow circles are FEM results for the continuum microstructure, while the solid points plotted in blue (dark gray) and green (light gray) are from two approaches of binary network mapping illustrated in the bottom insets. (b) Scaling analysis of the same data, with exponents s and t fitted over the range $0.03 \leq |p-p_c| \leq 0.2$; the values in parentheses are the exponents fitted on the whole curve.

[21]. We do not observe an additional percolation threshold at $p \approx 0.593$ [26] where connectivity through edges forms a percolating cluster; this represents an apparently minor improvement in connectivity as compared to the emergence of the first percolating path formed by both corner and edge contacts.

For comparison, we also map random checkerboards of the same size (100×100) to networks using the approach of Ref. [25], i.e., by assigning the four bonds surrounding corner contacts a third diffusivity $D_3 = \sqrt{D_1 D_2}$ and solving the Kirchhoff network equations to obtain D_{eff}. The results are shown in Fig. 2(a). Figure 2(a) also contains network results obtained from using a second mapping criterion, by which a corner contact transforms into a diagonal next-nearest-neighbor bond with diffusivity $D_3 = \sqrt{D_1 D_2}$. In agreement with prior studies that employed mapping [21,23–25], D_{eff} we find in Fig. 2(a) for both types of mapped networks exhibits a second percolation threshold $p_{c2} \approx 0.596$ in addition to the primary percolation transition at $p_{c1} \approx 0.41$. By comparison with the FEM continuum results, we conclude that this secondary threshold is an artifact of the mapping procedure.

Further reflection offers an explanation for the false second threshold introduced by mapping the continuum to a network. Specifically, mapping introduces an artificial third property scale, the geometric mean $\sqrt{D_1 D_2}$, for corner contacts; this in essence renders what should be a binary continuum problem a ternary network problem. Transport on three-component networks with $D_1 < D_3 < D_2$ has been shown to reveal two sets of percolation thresholds [29]: the first at $f_2 + f_3 = f_c$ and the second at $f_2 = f_c$, with f_c the bond percolation threshold for binary networks and the other f_i denoting the phase fractions of diffusivity D_i. These two sets of percolation thresholds reduce to two percolation thresholds when described in terms of the continuum phase fraction p. A further significant implication of this result is that many excess fictitious critical points will be introduced when geometrically more complex composites are represented by multicomponent networks.

In the mapping approach, the presence of more than one percolation threshold also makes it difficult to extract correct scaling exponents s and t, which characterize the divergence of D_{eff} as p_c is approached from below and above, respectively, i.e., $D_{\text{eff}} \propto (p_c - p)^{-s}$ for $p < p_c$ and $D_{\text{eff}} \propto (p - p_c)^t$ for $p > p_c$. For the network data presented in Fig. 2(a), the exponents fitted on the ranges $0.03 \leq |p-p_{c1}| \leq 0.2$ and $0.03 \leq |p-p_{c2}| \leq 0.2$ are $(s_1, t_1) \approx (1.17, 1.57)$ and

$(s_2, t_2) \approx (1.63, 1.21)$ for the first type of mapping (in blue) and are $(s_1, t_1) \approx (1.04, 1.74)$ and $(s_2, t_2) \approx (1.97, 1.20)$ for the second type of mapping (in green). It is not clear which among these exponents should be compared to the exponents established for lattice percolation in order to evaluate the universality. The continuum exponents extracted from the same range of phase fractions are $(s, t) \approx (1.25, 1.42)$, which are notably different from those obtained from the network results. As shown in Fig. 2(b), while s_1 and s might be considered equivalent exponents, neither t_1 nor t_2 is a good match to the continuum exponent t. These differences between the exponents in the network and continuum approaches further discourage the use of network mapping to study continuum percolation of effective properties. Furthermore, the continuum values of s and t are slightly asymmetric and are also slightly different from their lattice counterparts, which are symmetric with the value $s=t \approx 1.3$ [30]. Our data thus open the possibility that continuum transport percolation is not universal, and that the mapping approaches used in the literature that transform binary continua containing geometric irregularities into multicomponent network problems may generally find different critical scaling behaviors.

If, as we suggest above, the principal problem with conventional "ternary" mappings is the introduction of spurious secondary percolation thresholds, then an obvious remedy to this problem would be to find a binary mapping that does not introduce an artificial third component. We explore this possibility in Fig. 3(a) by using a mapping in which the four bonds surrounding a corner contact are assigned diffusivity D_2 (in blue). Although this mapping gives a percolation threshold at $p_c \approx 0.41$ similar to that from the FEM analysis on continuum microstructures, the resulting scaling exponent $t \approx 1.08$ is very different from the continuum result $t \approx 1.42$, as shown in Fig. 3(b). The other type of binary mapping whereby the four bonds surrounding a corner contact are instead assigned diffusivity D_1 does not lead to a matching percolation threshold or scaling exponent t, as shown in Fig. 3 (in green). The scaling exponent s for either network is similar to the continuum result; the specific treatment of connectivity across corner contacts mainly affects the scaling exponent t that characterizes D_{eff} above p_c.

We close by noting that, while we have focused much of our discussion here on corner contacts in continuum microstructures, we believe that similar considerations should apply to other microstructural features that lead to strong variations in the local flux and transport coefficients, such as overlapping spheres vs peripherally touching spheres, a distribution of neck widths in Swiss-cheese models [8,9,31,32], or conduction via tunneling processes [33,34]. This class of continuum percolation problems might be akin to systems where anomalous distributions of local transport coefficients induce nonuniversality [35,36]. We suggest that more studies are needed in which transport equations are explicitly solved on the continuum, in order to elucidate the universality of continuum percolation of transport properties.

This work was supported by the U.S. National Science Foundation under Contracts No. DMR-0346848 and No. DMR-0855402.

[1] I. C. Kim and S. Torquato, J. Appl. Phys. **69**, 2280 (1991).
[2] S. Torquato, *Random Heterogeneous Materials: Microstructure and Macroscopic Properties* (Springer, New York, 2002).
[3] D. R. Stevens, L. N. Downen, and L. I. Clarke, Phys. Rev. B **78**, 235425 (2008).
[4] A. A. Snarskii and M. I. Zhenirovskyy, Phys. Rev. E **78**, 021108 (2008).
[5] D. Sangare and P. M. Adler, Phys. Rev. E **79**, 052101 (2009).
[6] T. C. Choy, *Effective Medium Theory* (Clarendon Press, Oxford, 1999).
[7] I. Balberg, N. Binenbaum, and C. H. Anderson, Phys. Rev. Lett. **51**, 1605 (1983).
[8] S. Feng, B. I. Halperin, and P. N. Sen, Phys. Rev. B **35**, 197 (1987).
[9] B. I. Halperin, S. Feng, and P. N. Sen, Phys. Rev. Lett. **54**, 2391 (1985).
[10] J. Zhu, A. Jabini, K. M. Golden, H. Eicken, and M. Morris, Ann. Glaciol. **44**, 129 (2006).
[11] Y. Hakobyan, K. D. Papoulia, and M. D. Grigoriu, Phys. Rev. B **76**, 144205 (2007).
[12] R. V. Craster, Proc. R. Soc. London, Ser. A **456**, 2741 (2000).
[13] R. J. Duffin, Circuits Syst. Signal Process. **9**, 129 (1990).
[14] A. M. Dykhne, Sov. Phys. JETP **32**, 63 (1971).
[15] J. Helsing, Phys. Rev. B **44**, 11677 (1991).
[16] J. B. Keller, J. Math. Phys. **5**, 548 (1964).
[17] Y. V. Obnosov, Proc. R. Soc. London, Ser. A **452**, 2423 (1996).
[18] G. W. Milton, *The Theory of Composites* (Cambridge University Press, Cambridge, England, 2002).
[19] Z. Hashin and S. Shtrikman, J. Appl. Phys. **33**, 3125 (1962).
[20] Z. Hashin and S. Shtrikman, Phys. Rev. **130**, 129 (1963).
[21] P. Sheng and R. V. Kohn, Phys. Rev. B **26**, 1331 (1982).
[22] J. Koplik, *Homogenization and Effective Medium Methods for Transport in Disordered Granular Systems*, Physics of Granular Media (Nova, New York, 1991), p. 215.
[23] B. Nettelblad, E. Martensson, C. Onneby, U. Gafvert, and A. Gustafsson, J. Phys. D **36**, 399 (2003).
[24] E. Martensson and U. Gafvert, J. Phys. D **37**, 112 (2004).
[25] E. Martensson and U. Gafvert, J. Phys. D **36**, 1864 (2003).
[26] D. Stauffer and A. Aharony, *Introduction to Percolation Theory* (Taylor & Francis, London, 1992).
[27] I. V. Petrov, I. I. Stoynev, and F. V. Babalievskii, J. Phys. A **24**, 4421 (1991).
[28] K. Malarz and S. Galam, Phys. Rev. E **71**, 016125 (2005).
[29] Y. Chen and C. A. Schuh, Acta Mater. **54**, 4709 (2006).
[30] J. P. Clerc, G. Giraud, J. M. Laugier, and J. M. Luck, Adv. Phys. **39**, 191 (1990).
[31] L. Benguigui, Phys. Rev. B **34**, 8176 (1986).
[32] C. J. Lobb and M. G. Forrester, Phys. Rev. B **35**, 1899 (1987).
[33] C. Grimaldi and I. Balberg, Phys. Rev. Lett. **96**, 066602 (2006).
[34] N. Johner, C. Grimaldi, I. Balberg, and P. Ryser, Phys. Rev. B **77**, 174204 (2008).
[35] P. M. Kogut and J. P. Straley, J. Phys. C **12**, 2151 (1979).
[36] A. Bunde, H. Harder, and S. Havlin, Phys. Rev. B **34**, 3540 (1986).